

MIT Open Access Articles

Measurement of the Ξ ^[superscript -]_[subscript b] and Ω ^[superscript -]_[subscript b] Baryon Lifetimes

The MIT Faculty has made this article openly available. **Please share** how this access benefits you. Your story matters.

Citation: Aaij, R., et al. "Measurement of the Ξ ^[superscript -]_[subscript b] and Ω ^[superscript -]_[subscript b] Baryon Lifetimes." Physics Letters B, vol. 736, Sept. 2014, pp. 154–62. © 2014 The Authors

As Published: <http://dx.doi.org/10.1016/J.PHYSLETB.2014.06.064>

Publisher: Elsevier BV

Persistent URL: <http://hdl.handle.net/1721.1/116480>

Version: Final published version: final published article, as it appeared in a journal, conference proceedings, or other formally published context

Terms of use: Attribution 4.0 International (CC BY 4.0)





Measurement of the Ξ_b^- and Ω_b^- baryon lifetimes



LHCb Collaboration

ARTICLE INFO

Article history:

Received 7 May 2014

Received in revised form 18 June 2014

Accepted 23 June 2014

Available online 26 June 2014

Editor: W.-D. Schlatter

ABSTRACT

Using a data sample of pp collisions corresponding to an integrated luminosity of 3 fb^{-1} , the Ξ_b^- and Ω_b^- baryons are reconstructed in the $\Xi_b^- \rightarrow J/\psi \Xi^-$ and $\Omega_b^- \rightarrow J/\psi \Omega^-$ decay modes and their lifetimes measured to be

$$\tau(\Xi_b^-) = 1.55_{-0.09}^{+0.10} (\text{stat}) \pm 0.03 (\text{syst}) \text{ ps},$$

$$\tau(\Omega_b^-) = 1.54_{-0.21}^{+0.26} (\text{stat}) \pm 0.05 (\text{syst}) \text{ ps}.$$

These are the most precise determinations to date. Both measurements are in good agreement with previous experimental results and with theoretical predictions.

© 2014 The Authors. Published by Elsevier B.V. This is an open access article under the CC BY license (<http://creativecommons.org/licenses/by/3.0/>). Funded by SCOAP³.

1. Introduction

Heavy baryons are systems of three quarks, among which at least one is c or b . The quarks are bound by the strong interaction, which is described by quantum chromodynamics (QCD). Hadron lifetimes are among the most useful inputs to tune the parameters of QCD models. A powerful approach for theoretical predictions of b -hadron lifetime ratios is the heavy quark expansion (HQE) framework [1] which allows calculations in powers of Λ_{QCD}/m_b , where Λ_{QCD} is the energy scale at which QCD becomes non-perturbative and m_b is the b -quark mass. With the exception of the b hadrons containing a c quark, the predictions for the various b -hadron lifetimes only start to differ at the order $\Lambda_{\text{QCD}}^2/m_b^2$ and are equal within several percent.

So far only the most abundantly produced b baryon, the Λ_b^0 with quark content udb , has been studied in detail. Early Λ_b^0 lifetime measurements [2–5] yielded values significantly smaller than the B -meson lifetime determinations, casting doubt on the HQE and causing increased theoretical activity [6–11]. More recent determinations of the ratio between the Λ_b^0 and B^0 lifetimes, for instance that of Ref. [12], are in much better agreement with the original predictions. However, less information exists on the strange b baryons, which are less abundantly produced than Λ_b^0 baryons. In particular for the Ξ_b^- (dsb) and Ω_b^- (ssb) baryons only a few theoretical lifetime calculations are available [13,7,8]. Furthermore, most of the predictions date back to the 1990s and have limited precision, with central values ranging from 1.0 ps to 1.7 ps. New experimental data are needed to provide more stringent constraints on the models.

The weakly decaying Ξ_b^- and Ω_b^- baryons were observed for the first time at the Tevatron experiments CDF [14,15] and D0

[16,17]. Prior to these first observations, the average Ξ_b lifetime (including Ξ_b^- and Ξ_b^0) was measured by the LEP experiments DELPHI [18,19] and ALEPH [20] using partially reconstructed decays. So far the only exclusive lifetime measurement of the strange b baryons Ξ_b^- and Ω_b^- has been made by the CDF experiment [15, 21]. Recently, LHCb demonstrated its ability to reconstruct a significant number of Ξ_b^- and Ω_b^- baryons [22] and to measure precisely b -hadron lifetimes [23].

In this Letter we present lifetime measurements of the Ξ_b^- and Ω_b^- baryons reconstructed in the $\Xi_b^- \rightarrow J/\psi \Xi^-$ and $\Omega_b^- \rightarrow J/\psi \Omega^-$ decay modes. The daughter particles are reconstructed in the decay modes $J/\psi \rightarrow \mu^+ \mu^-$, $\Xi^- \rightarrow \Lambda \pi^-$, $\Omega^- \rightarrow \Lambda K^-$ and $\Lambda \rightarrow p \pi^-$. Unless specified otherwise, charge-conjugated states are implied throughout.

2. Detector and event samples

The LHCb detector [24] is a single-arm forward spectrometer covering the pseudorapidity range $2 < \eta < 5$, designed for the study of particles containing b or c quarks. The detector includes a high-precision tracking system consisting of a silicon-strip vertex detector surrounding the pp interaction region, a large-area silicon-strip detector located upstream of a dipole magnet with a bending power of about 4 Tm, and three stations of silicon-strip detectors and straw drift tubes [25] placed downstream of the magnet. The combined tracking system provides a momentum measurement with a relative uncertainty that varies from 0.4% at low momentum, p , to 0.6% at 100 GeV/ c , and an impact parameter measurement with a resolution of 20 μm for charged particles with large transverse momentum, p_T . Different types of charged hadrons are distinguished using information from

two ring-imaging Cherenkov detectors [26]. Photon, electron and hadron candidates are identified by a calorimeter system consisting of scintillating-pad and preshower detectors, an electromagnetic calorimeter and a hadronic calorimeter. Muons are identified by a system composed of alternating layers of iron and multiwire proportional chambers [27].

The trigger consists of a hardware stage, based on information from the calorimeter and muon systems, followed by a software stage, which applies a full event reconstruction. For this measurement, events are first required to pass the hardware trigger, which selects muons with high transverse momentum. In the subsequent software stage, events are retained by two independent sets of requirements. One demands a muon candidate with momentum larger than 6 GeV/c that, combined with another oppositely charged muon candidate, yields a dimuon mass larger than 2.7 GeV/c². The other requires a muon candidate with momentum larger than 8 GeV/c and an impact parameter above 100 μm with respect to all of the primary *pp* interaction vertices (PVs) in the event. Finally, for all candidates, two muons are required to form a vertex that is significantly displaced from the PVs.

The Ξ_b^- and Ω_b^- lifetime measurements presented here are based on the combination of the two data sets recorded in 2011 and 2012. During the year 2011 the LHCb detector recorded *pp* collisions at a centre-of-mass energy of $\sqrt{s} = 7$ TeV corresponding to an integrated luminosity of 1 fb⁻¹. In 2012, it recorded approximately twice as much data at $\sqrt{s} = 8$ TeV. Between 2011 and 2012, an improvement in the tracking algorithm of the vertex detector was introduced, leading to different trigger and reconstruction efficiencies in the two data sets. The polarity of the dipole magnet was periodically inverted so that roughly half of the data was collected with each polarity.

Four million Ξ_b^- (Ω_b^-) signal events, corresponding to approximately 135 fb⁻¹ (1700 fb⁻¹) of LHCb data, were simulated with each of the 2011 and 2012 data taking conditions. The *pp* collisions are generated using PYTHIA [28] with a specific LHCb configuration [29]. Decays of hadronic particles are described by EVTGEN [30], in which final state radiation is generated using PHOTOS [31]. The interaction of the generated particles with the detector and its response are implemented using the GEANT4 toolkit [32] as described in Ref. [33].

3. Reconstruction and selection

The $J/\psi \rightarrow \mu^+\mu^-$ decay is reconstructed from oppositely charged particles that leave deposits in the vertex detector, the tracking stations and the muon system. The hyperons in the *b*-baryon decay chains (Ξ^- , Ω^- and Λ) are long-lived; approximately 10% of all reconstructed *b*-baryon candidates are reconstructed with all tracks leaving deposits in the vertex detector. To retain as many candidates as possible, tracks that have no vertex detector information are also considered for the reconstruction of the hyperon decays.

The Ξ_b^- and Ω_b^- candidates are selected through identical requirements except for the ranges in which the baryon masses are reconstructed. In addition, for the Ω_b^- case the charged track from the Ω^- decay is required to be identified as a kaon by the particle identification detectors, removing more than 95% of the background pions.

All final-state tracks are required to satisfy minimal quality criteria and kinematic requirements. In order to reduce backgrounds from combinations of random tracks, the decay vertices are required to be well reconstructed. The J/ψ , Ξ^- , Ω^- and Λ candidates are selected within mass windows of ± 60 MeV/c², ± 11 MeV/c², ± 11 MeV/c² and ± 6 MeV/c², respectively, around the corresponding known masses [34].

The hadronic final-state tracks are required to have large impact parameters with respect to the PV associated with the *b*-baryon candidate. The associated PV is chosen as the PV giving the smallest increase in the χ^2 of the PV fit when the *b* baryon is included. The associated PV is also required to be isolated with respect to other PVs and consistent with the nominal interaction region.

The *b*-baryon mass is computed after a complete kinematic fit of the decay chain [35] in which the masses of both daughter particles are constrained to their known values [34]. No constraint is applied on the Λ mass. The resulting *b*-baryon invariant mass is required to lie in the range 5600–6000 MeV/c² for Ξ_b^- candidates and 5800–6300 MeV/c² for Ω_b^- candidates. The decay time of the *b*-baryon candidate, *t*, is computed from the decay length, *d*, as

$$t = \frac{d}{\beta\gamma c} = \frac{m}{p}d, \quad (1)$$

where *m* is the reconstructed mass and *p* the reconstructed momentum of the *b*-baryon candidate. The decay length itself is obtained from a refit of the decay chain with no mass constraints in order to keep the correlation between the reconstructed decay time and mass at a negligible level. Backgrounds are further suppressed by requiring this decay chain fit to be of good quality. The reconstructed decay time is required to lie in the range 0.3–14 ps. The lower bound of this decay-time range helps to suppress background coming from random combinations of tracks with real J/ψ mesons produced at the PV. In less than 1% of the cases, more than one candidate per event pass the selection criteria and only the candidate with the best decay chain fit result is retained.

4. Resolution and efficiency

The decay time resolution is obtained by fitting the difference between the reconstructed decay time, *t*, and the true decay time, *t*_{true}, in simulated events. The fit model is a single Gaussian function $G(t - t_{\text{true}}, \bar{t}, \sigma_{\text{res}})$ where the mean, \bar{t} , and the width, σ_{res} , are left free. For both considered decay modes and both data-taking periods, \bar{t} is compatible with zero and σ_{res} is close to 50 fs.

A bias in the measured lifetime can arise from a non-uniform efficiency as a function of the *b*-baryon decay time [23]. There are two types of inefficiencies which alter the decay time distribution. The first affects mostly candidates with small decay times and is induced by the requirements of the trigger that reject predominantly short-lived *b* baryons. The second affects mostly candidates with large decay times and is due to the geometrical detector acceptance, the reconstruction process and the selection criteria that lead to a lower efficiency for long-lived *b* baryons. Both effects are estimated and corrected for using simulation. This approach is validated with several techniques described in Section 6.

The two trigger selections used for these lifetime measurements include a requirement on the decay length significance of the J/ψ meson. In addition, one selection also contains a requirement on the impact parameter of the muons from the J/ψ decay. The two requirements induce an inefficiency at low values of the reconstructed decay time. To assess this effect, simulated events undergo an emulation of the trigger. In addition, an unbiased trigger selection is used to remove the contribution from the detector acceptance, the reconstruction and the selection. The resulting efficiency as a function of the reconstructed decay time is fitted with an empirical function of the form

$$\varepsilon_1(t) = \text{erf}(a \cdot (t - t_0)^n),$$

$$\text{where } \text{erf}(u) = \frac{2}{\sqrt{\pi}} \int_0^u e^{-x^2} dx, \quad (2)$$

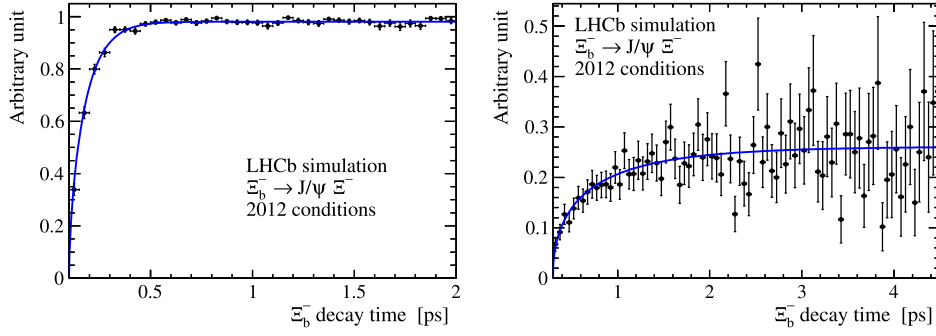


Fig. 1. Efficiency for triggering simulated Ξ_b^- events as a function of the reconstructed decay time under the 2012 data-taking conditions. Only a restricted decay-time range is shown in order to emphasize the region where the effect is large. The left panel shows the efficiency for events passing the trigger with only the requirement on the J/ψ vertex displacement. The right panel shows the efficiency for events passing the trigger with requirements on both the J/ψ vertex displacement and the muon impact parameter and required to not pass the other trigger. The results of fits with functions proportional to that given in Eq. (2) are overlaid.

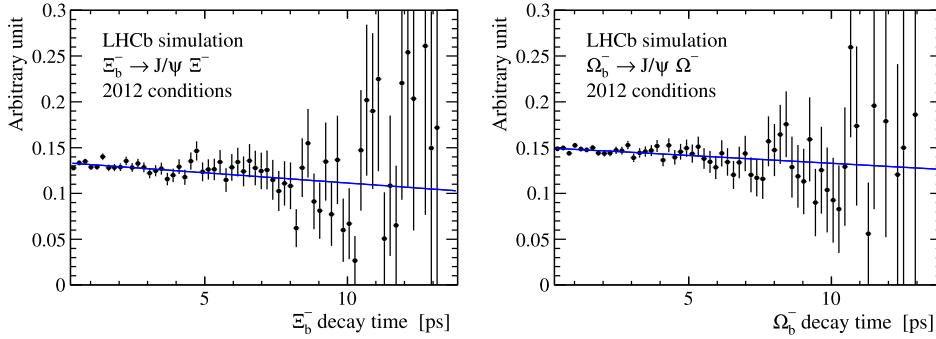


Fig. 2. Efficiency due to the detector acceptance, reconstruction and selection of simulated Ξ_b^- (left) and Ω_b^- (right) events as a function of the reconstructed decay time under the 2012 data-taking conditions. The results of fits with functions proportional to that given in Eq. (3) are overlaid.

Table 1

Fitted β values (in ps^{-1}) for the efficiency described in Eq. (3) extracted from simulated Ξ_b^- and Ω_b^- decays. The quoted uncertainties are statistical only.

Decay mode	2011 conditions	2012 conditions
$\Xi_b^- \rightarrow J/\psi \Xi^-$	$(-13.1 \pm 4.8) \times 10^{-3}$	$(-20.2 \pm 5.0) \times 10^{-3}$
$\Omega_b^- \rightarrow J/\psi \Omega^-$	$(-23.3 \pm 3.5) \times 10^{-3}$	$(-19.3 \pm 3.9) \times 10^{-3}$

and where a , t_0 and n are free parameters. The distributions of the decay products of the b baryons depend on the decay mode and on the year of data taking. This dependence slightly affects the shape of the efficiency as a function of the reconstructed decay time. Thus separate efficiency functions are obtained for the two decay modes, for the two data taking periods and for the two trigger selections. The efficiency functions corresponding to the 2012 data taking conditions for the Ξ_b^- case are shown in Fig. 1 as an example.

The dependence of the efficiency on the decay time due to the geometrical detector acceptance, the reconstruction and the selection is found to be well described with a linear function,

$$\varepsilon_2(t) = 1 + \beta t. \quad (3)$$

The free parameter β is obtained by fitting a function proportional to $\varepsilon_2(t) \cdot \int_0^\infty \exp(-t_{\text{true}}/\tau_{\text{gen}}) G(t - t_{\text{true}}, 0, \sigma_{\text{res}}) dt_{\text{true}}$ to the reconstructed decay time distribution of simulated signal events that are generated with a mean lifetime of τ_{gen} and that are fully reconstructed and selected. Separate values for β are determined for the two different decay modes and the two data-taking periods and are given in Table 1. The efficiency functions corresponding to the 2012 data taking conditions for the Ξ_b^- and Ω_b^- cases are shown in Fig. 2 as an example.

5. Lifetime fit

The lifetime is extracted from a two-dimensional extended maximum likelihood fit to the unbinned b -baryon mass and decay-time distributions. The mass and decay time are computed with the techniques described in Section 3. Assuming a negligible correlation between these two quantities, the two-dimensional probability density functions for the signal and the background are each written as the product of a mass term and a decay-time term.

For the mass distribution, the signal is described with a single Gaussian function in which the mean and width are free parameters. Independent means are used for the data recorded in 2011 and in 2012, since different calibrations are applied. The background in the mass distribution is modelled with an exponential function. The signal in the decay time distribution is described with the product of the efficiency functions (described in Eqs. (2) and (3)) and a convolution between an exponential function and a Gaussian function describing the decay time resolution,

$$S(t) = N \cdot \varepsilon_1(t) \cdot \varepsilon_2(t) \cdot \int_0^\infty e^{-t_{\text{true}}/\tau} G(t - t_{\text{true}}, 0, \sigma_{\text{res}}) dt_{\text{true}}, \quad (4)$$

where N is a normalisation parameter and τ the fitted lifetime. The decay time resolution σ_{res} is fixed to the value obtained in simulation, separately for each decay mode and each year of data taking. The background in the decay time distribution is modelled with the sum of two exponential functions that are also convolved with the fixed decay time resolution function. With the exception of σ_{res} , all background parameters are left free in the fit. A study based on pseudo-experiments shows that no observable bias to the measured lifetimes arises from the fit model itself.

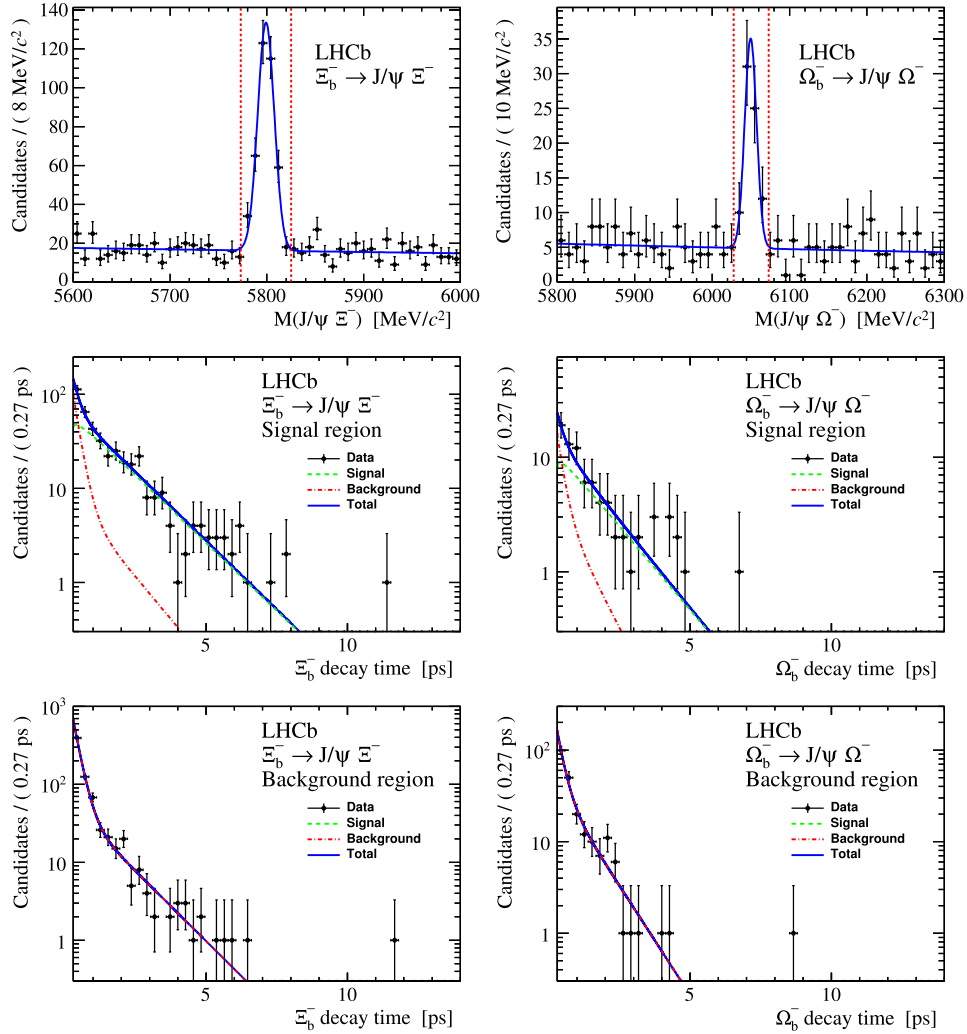


Fig. 3. Distributions of the reconstructed invariant mass (top) and decay time (middle and bottom) of the $\Xi_b^- \rightarrow J/\psi \Xi^-$ (left) and $\Omega_b^- \rightarrow J/\psi \Omega^-$ (right) candidates. The middle (bottom) panels show the decay time distributions of the candidates in the signal (background) mass regions. The signal mass region is defined as 5773–5825 MeV/c^2 for Ξ_b^- and 6028–6073 MeV/c^2 for Ω_b^- candidates, as shown by the vertical dotted lines in the mass distributions, whereas the background mass regions include all other candidates. The results of the fits are overlaid.

Table 2

Fitted parameters with statistical uncertainties for the Ξ_b^- and Ω_b^- signals.

Parameter	$\Xi_b^- \rightarrow J/\psi \Xi^-$	$\Omega_b^- \rightarrow J/\psi \Omega^-$
Signal yield	313 ± 20	58 ± 8
Mass resolution	$8.5 \pm 0.5 \text{ MeV}/c^2$	$7.5 \pm 1.0 \text{ MeV}/c^2$
Lifetime (τ)	$1.55^{+0.10}_{-0.09} \text{ ps}$	$1.54^{+0.26}_{-0.21} \text{ ps}$

The fit is performed for all selected b -baryon candidates. Due to the low signal yields, asymmetric uncertainties are calculated. Fig. 3 shows the invariant mass and decay time distributions and the projection of the fit results for the Ξ_b^- and Ω_b^- baryons. Table 2 displays the fit result for the relevant signal parameters.

As a consistency check for the fitting method, a measurement of the $\Lambda_b^0 \rightarrow J/\psi \Lambda$ lifetime is performed using the same data set and techniques as presented in this paper. The measured Λ_b^0 lifetime is consistent with the world average [34] and with recent measurements from LHCb [23,12].

6. Systematic uncertainties

Unless specified otherwise, the evaluation of the systematic uncertainties is performed by varying in turn each fixed parameter of

Table 3

Systematic uncertainties on the lifetime measurements in fs. For the total uncertainty, all the contributions are summed in quadrature.

Source	$\Xi_b^- \rightarrow J/\psi \Xi^-$	$\Omega_b^- \rightarrow J/\psi \Omega^-$
Trigger efficiency	9.9	6.5
Reconstruction and selection efficiency	29.0	45.0
Signal modelling	5.9	11.4
Combinatorial background modelling	3.0	3.0
Cross-feed background	0.1	11.1
Detector length scale	0.3	0.3
Total	31.4	48.3

the fit within its uncertainty and taking the change in the fit result. The total systematic uncertainty is obtained as the quadratic sum of the individual contributions. Distributions of results from fits to pseudo-experiments are used for the leading contributions (efficiencies and modelling) in order to ensure that they are not incorrectly estimated due to a statistical fluctuation of the data. A summary of all contributions to the total systematic uncertainty is given in Table 3.

Two contributions are considered as uncertainties due to the trigger efficiency. One arises from the finite size of the simulation

samples and is taken into account by varying the parameters of the efficiency function ε_1 within their uncertainties. The other is due to a potential discrepancy between data and simulation. This second contribution is assessed by repeating the fit using an efficiency obtained from a data sample of $B^0 \rightarrow J/\psi K_S^0$ decays that are topologically similar to the b -baryon decays of interest and reconstructed in data collected by the same trigger. In this case, extracting the efficiency from data is possible because a large sample, selected with triggers that do not bias the decay time distribution, is available (see Ref. [23]).

Two contributions are considered as uncertainties in determining the reconstruction and selection efficiency. One arises from the finite size of the simulation samples and is assessed by varying the parameter β within its statistical uncertainty. The other takes into account the quality of the simulation of the geometrical detector acceptance, the reconstruction process and the selection. For this second contribution, the β parameter is varied by $\pm 50\%$ to cover any possible discrepancy between data and simulation [36]. The total systematic uncertainty related to the reconstruction and selection efficiency, taken as the quadratic sum of the two contributions, is larger for Ω_b^- than for Ξ_b^- decays due to the larger value of the β parameter for Ω_b^- in 2011 data.

Several alternative fits are performed to assess the systematic uncertainties related to the signal modelling. In one fit, the Gaussian function describing the signal model in the b -baryon mass distribution is replaced by the sum of two Gaussian functions of common mean. The widths and the relative yields are left free. To assess the effect of the decay time resolution function, the widths of the corresponding Gaussian functions are varied by $\pm 10\%$. In another alternative fit, this resolution function is taken as the sum of two Gaussian functions instead of one, where the parameters are still taken from simulation. This takes into account potential tails in the decay time resolution distribution. All variations of the function describing the decay time resolution change the fit result by a negligible amount. Therefore the systematic uncertainty related to the signal modelling is dominated by the signal description in the mass distribution.

The systematic uncertainties due to combinatorial background are taken into account with three alternative fit models. In the first, the background in the mass distribution is described with a linear function. In another fit the background is modelled with two different exponential functions for the two different years of data taking. As an alternative description of the background in the decay time distribution, three exponential functions, instead of two, are convolved with the Gaussian resolution.

The only other significant background expected is a cross-feed between the two b -baryon decays. The rate and mass distribution of the cross-feed backgrounds is determined by reconstructing simulated decays of one channel under the hypothesis of the other. According to simulation, 0.24 (3.0) Ω_b^- (Ξ_b^-) decays are expected to be reconstructed as Ξ_b^- (Ω_b^-) over the full mass range. The effect of this background on the lifetime measurement is determined by injecting simulated background events into a fit of simulated signal events and taking the observed bias as the systematic uncertainty.

The overall length scale of the vertex detector is known with a relative precision of 0.02% [23]. As the measured decay length is directly proportional to the overall length scale, this precision directly translates into a relative uncertainty on the lifetime measurements.

7. Conclusion

Using data samples recorded during the years 2011 and 2012, corresponding to an integrated luminosity of 3 fb^{-1} , the lifetimes of the weakly decaying Ξ_b^- and Ω_b^- baryons are measured to be

$$\tau(\Xi_b^-) = 1.55_{-0.09}^{+0.10} (\text{stat}) \pm 0.03 (\text{syst}) \text{ ps},$$

$$\tau(\Omega_b^-) = 1.54_{-0.21}^{+0.26} (\text{stat}) \pm 0.05 (\text{syst}) \text{ ps}.$$

These are the most precise lifetime measurements of these b baryons to date. Both measurements are in agreement with the previous experimental results, in particular with the most recent ones from the CDF Collaboration of $\tau(\Xi_b^-) = 1.32 \pm 0.14 \text{ ps}$ and $\tau(\Omega_b^-) = 1.66 \pm 0.47 \text{ ps}$ [21]. The measurements also lie in the range predicted by theoretical calculations [13,7,8].

Acknowledgements

We express our gratitude to our colleagues in the CERN accelerator departments for the excellent performance of the LHC. We thank the technical and administrative staff at the LHCb institutes. We acknowledge support from CERN and from the national agencies: CAPES, CNPq, FAPERJ and FINEP (Brazil); NSFC (China); CNRS/IN2P3 and Region Auvergne (France); BMBF, DFG, HGF and MPG (Germany); SFI (Ireland); INFN (Italy); FOM and NWO (The Netherlands); SCSR (Poland); MEN/IFA (Romania); MinES, Rosatom, RFBR and NRC ‘‘Kurchatov Institute’’ (Russia); MinEco, XuntaGal and GENCAT (Spain); SNSF and SER (Switzerland); NASU (Ukraine); STFC and the Royal Society (United Kingdom); NSF (USA). We also acknowledge the support received from EPLANET, Marie Curie Actions and the ERC under FP7. The Tier1 computing centres are supported by IN2P3 (France), KIT and BMBF (Germany), INFN (Italy), NWO and SURF (The Netherlands), PIC (Spain), GridPP (United Kingdom). We are indebted to the communities behind the multiple open source software packages on which we depend. We are also thankful for the computing resources and the access to software R&D tools provided by Yandex LLC (Russia).

References

- [1] M. Neubert, *B decays and the heavy-quark expansion*, Adv. Ser. Dir. High Energy Phys. 15 (1998) 239, arXiv:hep-ph/9702375.
- [2] ALEPH Collaboration, D. Buskulic, et al., *Measurements of the b baryon lifetime*, Phys. Lett. B 357 (1995) 685.
- [3] OPAL Collaboration, R. Akers, et al., *A measurement of the Λ_b^0 lifetime*, Phys. Lett. B 353 (1995) 402.
- [4] DELPHI Collaboration, P. Abreu, et al., *Determination of the average lifetime of b baryons*, Z. Phys. C 71 (1996) 199.
- [5] CDF Collaboration, F. Abe, et al., *Measurement of Λ_b^0 lifetime using $\Lambda_b^0 \rightarrow \Lambda_c^+ l^- \bar{\nu}$* , Phys. Rev. Lett. 77 (1996) 1439.
- [6] G. Altarelli, et al., *Failure of local duality in inclusive non-leptonic heavy flavour*, Phys. Lett. B 382 (1996) 409, arXiv:hep-ph/9604202.
- [7] H.-Y. Cheng, *A phenomenological analysis of heavy hadron lifetimes*, Phys. Rev. D 56 (1997) 2783, arXiv:hep-ph/9704260.
- [8] T. Ito, M. Matsuda, Y. Matsui, *New possibility of solving the problem of lifetime ratio $\tau(\Lambda_b^0)/\tau(B_d)$* , Prog. Theor. Phys. 99 (1998) 271, arXiv:hep-ph/9705402.
- [9] N. Uraltsev, *Topics in the heavy quark expansion*, arXiv:hep-ph/0010328.
- [10] F. Gabbiani, A.I. Onishchenko, A.A. Petrov, *Λ_b^0 lifetime puzzle in heavy-quark expansion*, Phys. Rev. D 68 (2003) 114006, arXiv:hep-ph/0303235.
- [11] F. Gabbiani, A.I. Onishchenko, A.A. Petrov, *Spectator effects and lifetimes of heavy hadrons*, Phys. Rev. D 70 (2004) 094031, arXiv:hep-ph/0407004.
- [12] LHCb Collaboration, R. Aaij, et al., *Precision measurement of the ratio of the Λ_b^0 to \bar{B}^0 lifetimes*, Phys. Lett. B 734 (2014) 122, arXiv:1402.6242.
- [13] I.I. Bigi, *The QCD perspective on lifetimes of heavy-flavour hadrons*, arXiv:hep-ph/9508408.
- [14] CDF Collaboration, T. Aaltonen, et al., *Observation and mass measurement of the baryon Ξ_b^-* , Phys. Rev. Lett. 99 (2007) 052002, arXiv:0707.0589.
- [15] CDF Collaboration, T. Aaltonen, et al., *Observation of the Ω_b^- baryon and measurement of the properties of the Ξ_b^- and Ω_b^- baryons*, Phys. Rev. D 80 (2009) 072003, arXiv:0905.3123.

- [16] D0 Collaboration, V. Abazov, et al., Direct observation of the strange b baryon Ξ_b^- , Phys. Rev. Lett. 99 (2007) 052001, arXiv:0706.1690.
- [17] D0 Collaboration, V. Abazov, et al., Observation of the doubly strange b baryon Ω_b^- , Phys. Rev. Lett. 101 (2008) 232002, arXiv:0808.4142.
- [18] DELPHI Collaboration, P. Abreu, et al., Production of strange B baryons decaying into $\Xi^\mp - F^\mp$ pairs at LEP, Z. Phys. C 68 (1995) 541.
- [19] DELPHI Collaboration, J. Abdallah, et al., Production of Ξ_c^0 and Ξ_b^- in Z decays and lifetime measurement of Ξ_b , Eur. Phys. J. C 44 (2005) 299, arXiv:hep-ex/0510023.
- [20] ALEPH Collaboration, D. Buskulic, et al., Strange b baryon production and lifetime in Z decays, Phys. Lett. B 384 (1996) 449.
- [21] CDF Collaboration, T. Aaltonen, et al., Mass and lifetime measurements of bottom and charm baryons in $p\bar{p}$ collisions at $\sqrt{s} = 1.96$ TeV, Phys. Rev. D 89 (2014) 072014, arXiv:1403.8126.
- [22] LHCb Collaboration, R. Aaij, et al., Measurements of the Λ_b^0 , Ξ_b^- and Ω_b^- baryon masses, Phys. Rev. Lett. 110 (2013) 182001, arXiv:1302.1072.
- [23] LHCb Collaboration, R. Aaij, et al., Measurements of the B^+ , B^0 , B_s^0 meson and Λ_b^0 baryon lifetimes, J. High Energy Phys. 04 (2014) 114, arXiv:1402.2554.
- [24] LHCb Collaboration, A.A. Alves Jr., et al., The LHCb detector at the LHC, J. Instrum. 3 (2008) S08005.
- [25] R. Arink, et al., Performance of the LHCb outer tracker, J. Instrum. 9 (2014) P01002, arXiv:1311.3893.
- [26] M. Adinolfi, et al., Performance of the LHCb RICH detector at the LHC, Eur. Phys. J. C 73 (2013) 2431, arXiv:1211.6759.
- [27] A.A. Alves Jr., et al., Performance of the LHCb muon system, J. Instrum. 8 (2013) P02022, arXiv:1211.1346.
- [28] T. Sjöstrand, S. Mrenna, P. Skands, PYTHIA 6.4 physics and manual, J. High Energy Phys. 05 (2006) 026, arXiv:hep-ph/0603175; T. Sjöstrand, S. Mrenna, P. Skands, A brief introduction to PYTHIA 8.1, Comput. Phys. Commun. 178 (2008) 852, arXiv:0710.3820.
- [29] I. Belyaev, et al., Handling of the generation of primary events in Gauss, the LHCb simulation framework, in: Nuclear Science Symposium Conference Record (NSS/MIC), IEEE, 2010, p. 1155.
- [30] D.J. Lange, The EvtGen particle decay simulation package, Nucl. Instrum. Methods A 462 (2001) 152.
- [31] P. Golonka, Z. Was, PHOTOS Monte Carlo: a precision tool for QED corrections in Z and W decays, Eur. Phys. J. C 45 (2006) 97, arXiv:hep-ph/0506026.
- [32] Geant4 Collaboration, J. Allison, et al., Geant4 developments and applications, IEEE Trans. Nucl. Sci. 53 (2006) 270; Geant4 Collaboration, S. Agostinelli, et al., Geant4: a simulation toolkit, Nucl. Instrum. Methods A 506 (2003) 250.
- [33] M. Clemencic, et al., The LHCb simulation application, GAUSS: design, evolution and experience, J. Phys. Conf. Ser. 331 (2011) 032023.
- [34] Particle Data Group, J. Beringer, et al., Review of particle physics, Phys. Rev. D 86 (2012) 010001, and 2013 partial update for the 2014 edition.
- [35] W.D. Hulsbergen, Decay chain fitting with a Kalman filter, Nucl. Instrum. Methods A 552 (2005) 566, arXiv:physics/0503191.
- [36] LHCb Collaboration, R. Aaij, et al., Measurement of the CP -violating phase ϕ_s in the decay $B_s^0 \rightarrow J/\psi\phi$, Phys. Rev. Lett. 108 (2012) 101803, arXiv:1112.3183.

LHCb Collaboration

R. Aaij⁴¹, B. Adeva³⁷, M. Adinolfi⁴⁶, A. Affolder⁵², Z. Ajaltouni⁵, J. Albrecht⁹, F. Alessio³⁸, M. Alexander⁵¹, S. Ali⁴¹, G. Alkhazov³⁰, P. Alvarez Cartelle³⁷, A.A. Alves Jr^{25,38}, S. Amato², S. Amerio²², Y. Amhis⁷, L. An³, L. Anderlini^{17,g}, J. Anderson⁴⁰, R. Andreassen⁵⁷, M. Andreotti^{16,f}, J.E. Andrews⁵⁸, R.B. Appleby⁵⁴, O. Aquines Gutierrez¹⁰, F. Archilli³⁸, A. Artamonov³⁵, M. Artuso⁵⁹, E. Aslanides⁶, G. Auremma^{25,n}, M. Baalouch⁵, S. Bachmann¹¹, J.J. Back⁴⁸, A. Badalov³⁶, V. Balagura³¹, W. Baldini¹⁶, R.J. Barlow⁵⁴, C. Barschel³⁸, S. Barsuk⁷, W. Barter⁴⁷, V. Batozskaya²⁸, Th. Bauer⁴¹, A. Bay³⁹, J. Beddow⁵¹, F. Bedeschi²³, I. Bediaga¹, S. Belogurov³¹, K. Belous³⁵, I. Belyaev³¹, E. Ben-Haim⁸, G. Bencivenni¹⁸, S. Benson³⁸, J. Benton⁴⁶, A. Berezhnoy³², R. Bernet⁴⁰, M.-O. Bettler⁴⁷, M. van Beuzekom⁴¹, A. Bien¹¹, S. Bifani⁴⁵, T. Bird⁵⁴, A. Bizzeti^{17,i}, P.M. Bjørnstad⁵⁴, T. Blake⁴⁸, F. Blanc³⁹, J. Blouw¹⁰, S. Blusk⁵⁹, V. Bocci²⁵, A. Bondar³⁴, N. Bondar^{30,38}, W. Bonivento^{15,38}, S. Borghi⁵⁴, A. Borgia⁵⁹, M. Borsato⁷, T.J.V. Bowcock⁵², E. Bowen⁴⁰, C. Bozzi¹⁶, T. Brambach⁹, J. van den Brand⁴², J. Bressieux³⁹, D. Brett⁵⁴, M. Britsch¹⁰, T. Britton⁵⁹, N.H. Brook⁴⁶, H. Brown⁵², A. Bursche⁴⁰, G. Busetto^{22,q}, J. Buytaert³⁸, S. Cadeddu¹⁵, R. Calabrese^{16,f}, M. Calvi^{20,k}, M. Calvo Gomez^{36,o}, A. Camboni³⁶, P. Campana^{18,38}, D. Campora Perez³⁸, A. Carbone^{14,d}, G. Carboni^{24,l}, R. Cardinale^{19,38,j}, A. Cardini¹⁵, H. Carranza-Mejia⁵⁰, L. Carson⁵⁰, K. Carvalho Akiba², G. Casse⁵², L. Cassina²⁰, L. Castillo Garcia³⁸, M. Cattaneo³⁸, Ch. Cauet⁹, R. Cenci⁵⁸, M. Charles⁸, Ph. Charpentier³⁸, S.-F. Cheung⁵⁵, N. Chiapolini⁴⁰, M. Chrzaszcz^{40,26}, K. Ciba³⁸, X. Cid Vidal³⁸, G. Ciezarek⁵³, P.E.L. Clarke⁵⁰, M. Clemencic³⁸, H.V. Cliff⁴⁷, J. Closier³⁸, V. Coco³⁸, J. Cogan⁶, E. Cogneras⁵, P. Collins³⁸, A. Comerma-Montells¹¹, A. Contu^{15,38}, A. Cook⁴⁶, M. Coombes⁴⁶, S. Coquereau⁸, G. Corti³⁸, M. Corvo^{16,f}, I. Counts⁵⁶, B. Couturier³⁸, G.A. Cowan⁵⁰, D.C. Craik⁴⁸, M. Cruz Torres⁶⁰, S. Cunliffe⁵³, R. Currie⁵⁰, C. D'Ambrosio³⁸, J. Dalseno⁴⁶, P. David⁸, P.N.Y. David⁴¹, A. Davis⁵⁷, K. De Bruyn⁴¹, S. De Capua⁵⁴, M. De Cian¹¹, J.M. De Miranda¹, L. De Paula², W. De Silva⁵⁷, P. De Simone¹⁸, D. Decamp⁴, M. Deckenhoff⁹, L. Del Buono⁸, N. Déléage⁴, D. Derkach⁵⁵, O. Deschamps⁵, F. Dettori⁴², A. Di Canto³⁸, H. Dijkstra³⁸, S. Donleavy⁵², F. Dordei¹¹, M. Dorigo³⁹, A. Dosil Suárez³⁷, D. Dossett⁴⁸, A. Dovbnya⁴³, F. Dupertuis³⁹, P. Durante³⁸, R. Dzhelyadin³⁵, A. Dziurda²⁶, A. Dzyuba³⁰, S. Easo^{49,38}, U. Egede⁵³, V. Egorychev³¹, S. Eidelman³⁴, S. Eisenhardt⁵⁰, U. Eitschberger⁹, R. Ekelhof⁹, L. Eklund^{51,38}, I. El Rifai⁵, Ch. Elsasser⁴⁰, S. Esen¹¹, T. Evans⁵⁵, A. Falabella^{16,f}, C. Färber¹¹, C. Farinelli⁴¹, N. Farley⁴⁵, S. Farry⁵², D. Ferguson⁵⁰, V. Fernandez Albor³⁷, F. Ferreira Rodrigues¹, M. Ferro-Luzzi³⁸, S. Filippov³³, M. Fiore^{16,f}, M. Fiorini^{16,f}, M. Firlej²⁷, C. Fitzpatrick³⁸, T. Fiutowski²⁷, M. Fontana¹⁰, F. Fontanelli^{19,j}, R. Forty³⁸, O. Francisco², M. Frank³⁸, C. Frei³⁸, M. Frosini^{17,38,g}, J. Fu^{21,38}, E. Furfaro^{24,l}, A. Gallas Torreira³⁷, D. Galli^{14,d}, S. Gallorini²², S. Gambetta^{19,j}, M. Gandelman², P. Gandini⁵⁹, Y. Gao³, J. Garofoli⁵⁹, J. Garra Tico⁴⁷, L. Garrido³⁶, C. Gaspar³⁸, R. Gauld⁵⁵, L. Gavardi⁹, E. Gersabeck¹¹, M. Gersabeck⁵⁴, T. Gershon⁴⁸, Ph. Ghez⁴,

A. Gianelle²², S. Gianì³⁹, V. Gibson⁴⁷, L. Giubega²⁹, V.V. Gligorov³⁸, C. Göbel⁶⁰, D. Golubkov³¹,
 A. Golutvin^{53,31,38}, A. Gomes^{1,a}, H. Gordon³⁸, C. Gotti²⁰, M. Grabalosa Gándara⁵, R. Graciani Diaz³⁶,
 L.A. Granado Cardoso³⁸, E. Graugés³⁶, G. Graziani¹⁷, A. Grecu²⁹, E. Greening⁵⁵, S. Gregson⁴⁷,
 P. Griffith⁴⁵, L. Grillo¹¹, O. Grünberg⁶², B. Gui⁵⁹, E. Gushchin³³, Yu. Guz^{35,38}, T. Gys³⁸,
 C. Hadjivasiliou⁵⁹, G. Haefeli³⁹, C. Haen³⁸, S.C. Haines⁴⁷, S. Hall⁵³, B. Hamilton⁵⁸, T. Hampson⁴⁶,
 X. Han¹¹, S. Hansmann-Menzemer¹¹, N. Harnew⁵⁵, S.T. Harnew⁴⁶, J. Harrison⁵⁴, T. Hartmann⁶²,
 J. He³⁸, T. Head³⁸, V. Heijne⁴¹, K. Hennessy⁵², P. Henrard⁵, L. Henry⁸, J.A. Hernando Morata³⁷,
 E. van Herwijnen³⁸, M. Heß⁶², A. Hicheur¹, D. Hill⁵⁵, M. Hoballah⁵, C. Hombach⁵⁴, W. Hulsbergen⁴¹,
 P. Hunt⁵⁵, N. Hussain⁵⁵, D. Hutchcroft⁵², D. Hynds⁵¹, M. Idzik²⁷, P. Ilten⁵⁶, R. Jacobsson³⁸, A. Jaeger¹¹,
 J. Jalocha⁵⁵, E. Jans⁴¹, P. Jaton³⁹, A. Jawahery⁵⁸, M. Jezabek²⁶, F. Jing³, M. John⁵⁵, D. Johnson⁵⁵,
 C.R. Jones⁴⁷, C. Joram³⁸, B. Jost³⁸, N. Jurik⁵⁹, M. Kaballo⁹, S. Kandybei⁴³, W. Kanso⁶, M. Karacson³⁸,
 T.M. Karbach³⁸, M. Kelsey⁵⁹, I.R. Kenyon⁴⁵, T. Ketel⁴², B. Khanji²⁰, C. Khurewathanakul³⁹, S. Klaver⁵⁴,
 O. Kochebina⁷, M. Kolpin¹¹, I. Komarov³⁹, R.F. Koopman⁴², P. Koppenburg^{41,38}, M. Korolev³²,
 A. Kozlinskiy⁴¹, L. Kravchuk³³, K. Kreplin¹¹, M. Kreps⁴⁸, G. Krocker¹¹, P. Krokovny³⁴, F. Kruse⁹,
 M. Kucharczyk^{20,26,38,k}, V. Kudryavtsev³⁴, K. Kurek²⁸, T. Kvaratskheliya³¹, V.N. La Thi³⁹, D. Lacarrere³⁸,
 G. Lafferty⁵⁴, A. Lai¹⁵, D. Lambert⁵⁰, R.W. Lambert⁴², E. Lanciotti³⁸, G. Lanfranchi¹⁸, C. Langenbruch³⁸,
 B. Langhans³⁸, T. Latham⁴⁸, C. Lazzeroni⁴⁵, R. Le Gac⁶, J. van Leerdam⁴¹, J.-P. Lees⁴, R. Lefèvre⁵,
 A. Leflat³², J. Lefrançois⁷, S. Leo²³, O. Leroy⁶, T. Lesiak²⁶, B. Leverington¹¹, Y. Li³, M. Liles⁵²,
 R. Lindner³⁸, C. Linn³⁸, F. Lionetto⁴⁰, B. Liu¹⁵, G. Liu³⁸, S. Lohn³⁸, I. Longstaff⁵¹, J.H. Lopes²,
 N. Lopez-March³⁹, P. Lowdon⁴⁰, H. Lu³, D. Lucchesi^{22,q}, H. Luo⁵⁰, A. Lupato²², E. Luppi^{16,f},
 O. Lupton⁵⁵, F. Machefert⁷, I.V. Machikhiliyan³¹, F. Maciuc²⁹, O. Maev³⁰, S. Malde⁵⁵, G. Manca^{15,e},
 G. Mancinelli⁶, M. Manzali^{16,f}, J. Maratas⁵, J.F. Marchand⁴, U. Marconi¹⁴, C. Marin Benito³⁶,
 P. Marino^{23,s}, R. Märki³⁹, J. Marks¹¹, G. Martellotti²⁵, A. Martens⁸, A. Martín Sánchez⁷,
 M. Martinelli⁴¹, D. Martinez Santos⁴², F. Martinez Vidal⁶⁴, D. Martins Tostes², A. Massafferri¹,
 R. Matev³⁸, Z. Mathe³⁸, C. Matteuzzi²⁰, A. Mazurov^{16,f}, M. McCann⁵³, J. McCarthy⁴⁵, A. McNab⁵⁴,
 R. McNulty¹², B. McSkelly⁵², B. Meadows^{57,55}, F. Meier⁹, M. Meissner¹¹, M. Merk⁴¹, D.A. Milanes⁸,
 M.-N. Minard⁴, N. Moggi¹⁴, J. Molina Rodriguez⁶⁰, S. Monteil⁵, D. Moran⁵⁴, M. Morandin²²,
 P. Morawski²⁶, A. Mordà⁶, M.J. Morello^{23,s}, J. Moron²⁷, R. Mountain⁵⁹, F. Muheim⁵⁰, K. Müller⁴⁰,
 R. Muresan²⁹, M. Mussini¹⁴, B. Muster³⁹, P. Naik⁴⁶, T. Nakada³⁹, R. Nandakumar⁴⁹, I. Nasteva²,
 M. Needham⁵⁰, N. Neri²¹, S. Neubert³⁸, N. Neufeld³⁸, M. Neuner¹¹, A.D. Nguyen³⁹, T.D. Nguyen³⁹,
 C. Nguyen-Mau^{39,p}, M. Nicol⁷, V. Niess⁵, R. Niet⁹, N. Nikitin³², T. Nikodem¹¹, A. Novoselov³⁵,
 A. Oblakowska-Mucha²⁷, V. Obraztsov³⁵, S. Oggero⁴¹, S. Ogilvy⁵¹, O. Okhrimenko⁴⁴, R. Oldeman^{15,e},
 G. Onderwater⁶⁵, M. Orlandea²⁹, J.M. Otalora Goicochea², P. Owen⁵³, A. Oyanguren⁶⁴, B.K. Pal⁵⁹,
 A. Palano^{13,c}, F. Palombo^{21,t}, M. Palutan¹⁸, J. Panman³⁸, A. Papanestis^{49,38}, M. Pappagallo⁵¹,
 C. Parkes⁵⁴, C.J. Parkinson⁹, G. Passaleva¹⁷, G.D. Patel⁵², M. Patel⁵³, C. Patrignani^{19,j},
 A. Pazos Alvarez³⁷, A. Pearce⁵⁴, A. Pellegrino⁴¹, M. Pepe Altarelli³⁸, S. Perazzini^{14,d}, E. Perez Trigo³⁷,
 P. Perret⁵, M. Perrin-Terrin⁶, L. Pescatore⁴⁵, E. Pesen⁶⁶, K. Petridis⁵³, A. Petrolini^{19,j},
 E. Picatoste Olloqui³⁶, B. Pietrzyk⁴, T. Pilař⁴⁸, D. Pinci²⁵, A. Pistone¹⁹, S. Playfer⁵⁰, M. Plo Casasus³⁷,
 F. Polci⁸, A. Poluektov^{48,34}, E. Polcarpo², A. Popov³⁵, D. Popov¹⁰, B. Popovici²⁹, C. Potterat²,
 A. Powell⁵⁵, J. Prisciandaro³⁹, A. Pritchard⁵², C. Prouve⁴⁶, V. Pugatch⁴⁴, A. Puig Navarro³⁹, G. Punzi^{23,r},
 W. Qian⁴, B. Rachwal²⁶, J.H. Rademacker⁴⁶, B. Rakotomiramanana³⁹, M. Rama¹⁸, M.S. Rangel²,
 I. Raniuk⁴³, N. Rauschmayr³⁸, G. Raven⁴², S. Reichert⁵⁴, M.M. Reid⁴⁸, A.C. dos Reis¹, S. Ricciardi⁴⁹,
 A. Richards⁵³, M. Rihl³⁸, K. Rinnert⁵², V. Rives Molina³⁶, D.A. Roa Romero⁵, P. Robbe⁷, A.B. Rodrigues¹,
 E. Rodrigues⁵⁴, P. Rodriguez Perez⁵⁴, S. Roiser³⁸, V. Romanovsky³⁵, A. Romero Vidal³⁷, M. Rotondo²²,
 J. Rouvinet³⁹, T. Ruf³⁸, F. Ruffini²³, H. Ruiz³⁶, P. Ruiz Valls⁶⁴, G. Sabatino^{25,l}, J.J. Saborido Silva³⁷,
 N. Sagidova³⁰, P. Sail⁵¹, B. Saitta^{15,e}, V. Salustino Guimaraes², C. Sanchez Mayordomo⁶⁴,
 B. Sanmartin Sedes³⁷, R. Santacesaria²⁵, C. Santamarina Rios³⁷, E. Santovetti^{24,l}, M. Sapunov⁶,
 A. Sarti^{18,m}, C. Satriano^{25,n}, A. Satta²⁴, M. Savrie^{16,f}, D. Savrina^{31,32}, M. Schiller⁴², H. Schindler³⁸,
 M. Schlupp⁹, M. Schmelling¹⁰, B. Schmidt³⁸, O. Schneider^{39,*}, A. Schopper³⁸, M.-H. Schune⁷,
 R. Schwemmer³⁸, B. Sciascia¹⁸, A. Sciubba²⁵, M. Seco³⁷, A. Semennikov³¹, K. Senderowska²⁷, I. Sepp⁵³,
 N. Serra⁴⁰, J. Serrano⁶, L. Sestini²², P. Seyfert¹¹, M. Shapkin³⁵, I. Shapoval^{16,43,f}, Y. Shcheglov³⁰,
 T. Shears⁵², L. Shekhtman³⁴, V. Shevchenko⁶³, A. Shires⁹, R. Silva Coutinho⁴⁸, G. Simi²², M. Sirendi⁴⁷,

N. Skidmore⁴⁶, T. Skwarnicki⁵⁹, N.A. Smith⁵², E. Smith^{55,49}, E. Smith⁵³, J. Smith⁴⁷, M. Smith⁵⁴, H. Snoek⁴¹, M.D. Sokoloff⁵⁷, F.J.P. Soler⁵¹, F. Soomro³⁹, D. Souza⁴⁶, B. Souza De Paula², B. Spaan⁹, A. Sparkes⁵⁰, F. Spinella²³, P. Spradlin⁵¹, F. Stagni³⁸, S. Stahl¹¹, O. Steinkamp⁴⁰, O. Stenyakin³⁵, S. Stevenson⁵⁵, S. Stoica²⁹, S. Stone⁵⁹, B. Storaci⁴⁰, S. Stracka^{23,38}, M. Straticiuc²⁹, U. Straumann⁴⁰, R. Stroili²², V.K. Subbiah³⁸, L. Sun⁵⁷, W. Sutcliffe⁵³, K. Swientek²⁷, S. Swientek⁹, V. Syropoulos⁴², M. Szczekowski²⁸, P. Szczypka^{39,38}, D. Szilard², T. Szumlak²⁷, S. T'Jampens⁴, M. Teklishyn⁷, G. Tellarini^{16,f}, F. Teubert³⁸, C. Thomas⁵⁵, E. Thomas³⁸, J. van Tilburg⁴¹, V. Tisserand⁴, M. Tobin³⁹, S. Tolck⁴², L. Tomassetti^{16,f}, D. Tonelli³⁸, S. Topp-Joergensen⁵⁵, N. Torr⁵⁵, E. Tournefier⁴, S. Tourneur³⁹, M.T. Tran³⁹, M. Tresch⁴⁰, A. Tsaregorodtsev⁶, P. Tsopelas⁴¹, N. Tuning⁴¹, M. Ubeda Garcia³⁸, A. Ukleja²⁸, A. Ustyuzhanin⁶³, U. Uwer¹¹, V. Vagnoni¹⁴, G. Valenti¹⁴, A. Vallier⁷, R. Vazquez Gomez¹⁸, P. Vazquez Regueiro³⁷, C. Vázquez Sierra³⁷, S. Vecchi¹⁶, J.J. Velthuis⁴⁶, M. Veltri^{17,h}, G. Veneziano³⁹, M. Vesterinen¹¹, B. Viaud⁷, D. Vieira², M. Vieites Diaz³⁷, X. Vilasis-Cardona^{36,o}, A. Vollhardt⁴⁰, D. Volyanskyy¹⁰, D. Voong⁴⁶, A. Vorobyev³⁰, V. Vorobyev³⁴, C. Voß⁶², H. Voss¹⁰, J.A. de Vries⁴¹, R. Waldi⁶², C. Wallace⁴⁸, R. Wallace¹², J. Walsh²³, S. Wandernoth¹¹, J. Wang⁵⁹, D.R. Ward⁴⁷, N.K. Watson⁴⁵, D. Websdale⁵³, M. Whitehead⁴⁸, J. Wicht³⁸, D. Wiedner¹¹, G. Wilkinson⁵⁵, M.P. Williams⁴⁵, M. Williams⁵⁶, F.F. Wilson⁴⁹, J. Wimberley⁵⁸, J. Wishahi⁹, W. Wislicki²⁸, M. Witek²⁶, G. Wormser⁷, S.A. Wotton⁴⁷, S. Wright⁴⁷, S. Wu³, K. Wyllie³⁸, Y. Xie⁶¹, Z. Xing⁵⁹, Z. Xu³⁹, Z. Yang³, X. Yuan³, O. Yushchenko³⁵, M. Zangoli¹⁴, M. Zavertyaev^{10,b}, F. Zhang³, L. Zhang⁵⁹, W.C. Zhang¹², Y. Zhang³, A. Zhelezov¹¹, A. Zhokhov³¹, L. Zhong³, A. Zvyagin³⁸

¹ Centro Brasileiro de Pesquisas Físicas (CBPF), Rio de Janeiro, Brazil

² Universidade Federal do Rio de Janeiro (UFRJ), Rio de Janeiro, Brazil

³ Center for High Energy Physics, Tsinghua University, Beijing, China

⁴ LAPP, Université de Savoie, CNRS/IN2P3, Annecy-Le-Vieux, France

⁵ Clermont Université, Université Blaise Pascal, CNRS/IN2P3, LPC, Clermont-Ferrand, France

⁶ CPPM, Aix-Marseille Université, CNRS/IN2P3, Marseille, France

⁷ LAL, Université Paris-Sud, CNRS/IN2P3, Orsay, France

⁸ LPNHE, Université Pierre et Marie Curie, Université Paris Diderot, CNRS/IN2P3, Paris, France

⁹ Fakultät Physik, Technische Universität Dortmund, Dortmund, Germany

¹⁰ Max-Planck-Institut für Kernphysik (MPIK), Heidelberg, Germany

¹¹ Physikalisches Institut, Ruprecht-Karls-Universität Heidelberg, Heidelberg, Germany

¹² School of Physics, University College Dublin, Dublin, Ireland

¹³ Sezione INFN di Bari, Bari, Italy

¹⁴ Sezione INFN di Bologna, Bologna, Italy

¹⁵ Sezione INFN di Cagliari, Cagliari, Italy

¹⁶ Sezione INFN di Ferrara, Ferrara, Italy

¹⁷ Sezione INFN di Firenze, Firenze, Italy

¹⁸ Laboratori Nazionali dell'INFN di Frascati, Frascati, Italy

¹⁹ Sezione INFN di Genova, Genova, Italy

²⁰ Sezione INFN di Milano Bicocca, Milano, Italy

²¹ Sezione INFN di Milano, Milano, Italy

²² Sezione INFN di Padova, Padova, Italy

²³ Sezione INFN di Pisa, Pisa, Italy

²⁴ Sezione INFN di Roma Tor Vergata, Roma, Italy

²⁵ Sezione INFN di Roma La Sapienza, Roma, Italy

²⁶ Henryk Niewodniczanski Institute of Nuclear Physics Polish Academy of Sciences, Kraków, Poland

²⁷ AGH – University of Science and Technology, Faculty of Physics and Applied Computer Science, Kraków, Poland

²⁸ National Center for Nuclear Research (NCBJ), Warsaw, Poland

²⁹ Horia Hulubei National Institute of Physics and Nuclear Engineering, Bucharest-Magurele, Romania

³⁰ Petersburg Nuclear Physics Institute (PNPI), Gatchina, Russia

³¹ Institute of Theoretical and Experimental Physics (ITEP), Moscow, Russia

³² Institute of Nuclear Physics, Moscow State University (SINP MSU), Moscow, Russia

³³ Institute for Nuclear Research of the Russian Academy of Sciences (INR RAN), Moscow, Russia

³⁴ Budker Institute of Nuclear Physics (SB RAS) and Novosibirsk State University, Novosibirsk, Russia

³⁵ Institute for High Energy Physics (IHEP), Protvino, Russia

³⁶ Universitat de Barcelona, Barcelona, Spain

³⁷ Universidad de Santiago de Compostela, Santiago de Compostela, Spain

³⁸ European Organization for Nuclear Research (CERN), Geneva, Switzerland

³⁹ Ecole Polytechnique Fédérale de Lausanne (EPFL), Lausanne, Switzerland

⁴⁰ Physik-Institut, Universität Zürich, Zürich, Switzerland

⁴¹ Nikhef National Institute for Subatomic Physics, Amsterdam, The Netherlands

⁴² Nikhef National Institute for Subatomic Physics and VU University Amsterdam, Amsterdam, The Netherlands

⁴³ NSC Kharkiv Institute of Physics and Technology (NSC KIPT), Kharkiv, Ukraine

⁴⁴ Institute for Nuclear Research of the National Academy of Sciences (KINR), Kyiv, Ukraine

⁴⁵ University of Birmingham, Birmingham, United Kingdom

⁴⁶ H.H. Wills Physics Laboratory, University of Bristol, Bristol, United Kingdom

⁴⁷ Cavendish Laboratory, University of Cambridge, Cambridge, United Kingdom

⁴⁸ Department of Physics, University of Warwick, Coventry, United Kingdom

⁴⁹ STFC Rutherford Appleton Laboratory, Didcot, United Kingdom

⁵⁰ School of Physics and Astronomy, University of Edinburgh, Edinburgh, United Kingdom

- ⁵¹ School of Physics and Astronomy, University of Glasgow, Glasgow, United Kingdom
⁵² Oliver Lodge Laboratory, University of Liverpool, Liverpool, United Kingdom
⁵³ Imperial College London, London, United Kingdom
⁵⁴ School of Physics and Astronomy, University of Manchester, Manchester, United Kingdom
⁵⁵ Department of Physics, University of Oxford, Oxford, United Kingdom
⁵⁶ Massachusetts Institute of Technology, Cambridge, MA, United States
⁵⁷ University of Cincinnati, Cincinnati, OH, United States
⁵⁸ University of Maryland, College Park, MD, United States
⁵⁹ Syracuse University, Syracuse, NY, United States
⁶⁰ Pontifícia Universidade Católica do Rio de Janeiro (PUC-Rio), Rio de Janeiro, Brazil ^u
⁶¹ Institute of Particle Physics, Central China Normal University, Wuhan, Hubei, China ^v
⁶² Institut für Physik, Universität Rostock, Rostock, Germany ^w
⁶³ National Research Centre Kurchatov Institute, Moscow, Russia ^x
⁶⁴ Instituto de Física Corpuscular (IFIC), Universitat de Valencia-CSIC, Valencia, Spain ^y
⁶⁵ KVI – University of Groningen, Groningen, The Netherlands ^z
⁶⁶ Celal Bayar University, Manisa, Turkey ^{aa}

* Corresponding author.

- ^a Universidade Federal do Triângulo Mineiro (UFTRM), Uberaba-MG, Brazil.
^b P.N. Lebedev Physical Institute, Russian Academy of Science (LPI RAS), Moscow, Russia.
^c Università di Bari, Bari, Italy.
^d Università di Bologna, Bologna, Italy.
^e Università di Cagliari, Cagliari, Italy.
^f Università di Ferrara, Ferrara, Italy.
^g Università di Firenze, Firenze, Italy.
^h Università di Urbino, Urbino, Italy.
ⁱ Università di Modena e Reggio Emilia, Modena, Italy.
^j Università di Genova, Genova, Italy.
^k Università di Milano Bicocca, Milano, Italy.
^l Università di Roma Tor Vergata, Roma, Italy.
^m Università di Roma La Sapienza, Roma, Italy.
ⁿ Università della Basilicata, Potenza, Italy.
^o LIFAELS, La Salle, Universitat Ramon Llull, Barcelona, Spain.
^p Hanoi University of Science, Hanoi, Viet Nam.
^q Università di Padova, Padova, Italy.
^r Università di Pisa, Pisa, Italy.
^s Scuola Normale Superiore, Pisa, Italy.
^t Università degli Studi di Milano, Milano, Italy.
^u Associated to Universidade Federal do Rio de Janeiro (UFRJ), Rio de Janeiro, Brazil.
^v Associated to Center for High Energy Physics, Tsinghua University, Beijing, China.
^w Associated to Physikalisches Institut, Ruprecht-Karls-Universität Heidelberg, Heidelberg, Germany.
^x Associated to Institute of Theoretical and Experimental Physics (ITEP), Moscow, Russia.
^y Associated to Universitat de Barcelona, Barcelona, Spain.
^z Associated to Nikhef National Institute for Subatomic Physics, Amsterdam, The Netherlands.
^{aa} Associated to European Organization for Nuclear Research (CERN), Geneva, Switzerland.